

# Lysophospholipid receptors LPA<sub>1-3</sub> are not required for the inhibitory effects of LPA on mouse retinal growth cones

Eric Birgbauer  
Jerold Chun

Department of Molecular Biology,  
Helen L Dorris Institute for  
Neurological and Psychiatric  
Disorders, The Scripps Research  
Institute, La Jolla, CA, USA

**Abstract:** One of the major requirements in the development of the visual system is axonal guidance of retinal ganglion cells toward correct targets in the brain. A novel class of extracellular lipid signaling molecules, lysophospholipids, may serve as potential axon guidance cues. They signal through cognate G protein-coupled receptors, at least some of which are expressed in the visual system. Here we show that in the mouse visual system, a lysophospholipid known as lysophosphatidic acid (LPA) is inhibitory to retinal neurites in vitro when delivered extracellularly, causing growth cone collapse and neurite retraction. This inhibitory effect of LPA is both active in the nanomolar range and specific compared to the related lysophospholipid, sphingosine 1-phosphate (S1P). Knockout mice lacking three of the five known LPA receptors, LPA<sub>1-3</sub>, continue to display retinal growth cone collapse and neurite retraction in response to LPA, demonstrating that these three receptors are not required for these inhibitory effects and indicating the existence of one or more functional LPA receptors expressed on mouse retinal neurites that can mediate neurite retraction.

**Keywords:** retinal ganglion cells, lysophosphatidic acid, axon guidance

## Introduction

During development, the visual system forms by a self-wiring mechanism where axons extend from retinal ganglion cells (RGCs) in the eye and grow through intervening tissue to connect to targets in the brain. Even in the complex vertebrate nervous system, these connections are precise and not random. This precision is due to specific guidance of axons to the lateral geniculate nucleus (LGN) and superior colliculus (or optic tectum) followed by pruning mechanisms that further refine the patterns of connections, resulting in a precise topographic map.<sup>1-4</sup> During development, the first step in this process is the specific guidance of axons to their targets. Studies have uncovered some of the molecular cues that RGC axons use, as well as the responding receptors, and progress has been made in defining the roles of protein cues, such as semaphorins, ephrins, netrins, slits, and CAMs.<sup>2,5</sup> Some of these cues are attractive for axonal growth cones, while others are inhibitory; intriguingly, many of these guidance interactions appear to be inhibitory.

In recent years, the roles of an interesting new class of biologically active molecules, lysophospholipids, has begun to be unveiled. These lysophospholipids are derived from membrane phospholipids that, as a class, represent a major constituent of the brain.<sup>6-8</sup> Two major forms of lysophospholipids are lysophosphatidic acid (LPA) and sphingosine 1-phosphate (S1P), both of which have been shown to have effects in the nervous system and development, as well as cancer, cell proliferation, apoptosis, and angiogenesis.<sup>6,8-12</sup>

Correspondence: Eric Birgbauer  
Department of Biology, Winthrop  
University, Rock Hill, SC 29733, USA  
Tel +1 803 323 2111 ext 6288  
Fax +1 803 323 3448  
Email birgbauere@winthrop.edu

In the nervous system, evidence has accumulated for roles of LPA and S1P in cortical development, myelination, pain, hyperexcitability, and axon growth.<sup>12–15</sup> Similar to many of the inhibitory protein axon guidance cues, LPA and S1P have been shown to be inhibitory *in vitro* to neural cell lines, as well as some primary neurons, often causing growth cone collapse and neurite retraction.<sup>16–27</sup> As such, these lysophospholipids are potential candidates for guiding retinal axons during development.

The lysophospholipids function as extracellular signaling molecules by binding to cell surface receptors. The receptors for LPA and S1P have been identified as members of the G protein-coupled receptor (GPCR) family.<sup>8,9,28–31</sup> (Intriguingly from a biomedical perspective, since there has been great success in targeting GPCRs for pharmacological interventions in human disease,<sup>6,32,33</sup> pharmacological agents against lysophospholipid receptors could lead to efficacious medical treatments.) For the lysophospholipids LPA and S1P, there have been five receptors identified for LPA, named LPA<sub>1</sub> to LPA<sub>5</sub>, and five receptors for S1P, S1P<sub>1</sub> to S1P<sub>5</sub>.<sup>30,34–36</sup> Of the LPA receptors, the first three identified, LPA<sub>1–3</sub>, are homologous,<sup>30,37–39</sup> while the more recently identified LPA receptors LPA<sub>4</sub> and LPA<sub>5</sub> are less closely related.<sup>34–36</sup> Furthermore, there has been considerable characterization of the intracellular signaling pathways downstream of LPA receptors.<sup>7,40,41</sup> For example, in neural cell lines, a major receptor-mediated cellular response to LPA is process retraction, which signals through rho via the heterotrimeric G protein subunit G $\alpha_{12/13}$ .<sup>28,42</sup>

The mouse visual system is well characterized for its development and axonal pathfinding.<sup>2,5,43</sup> Here we demonstrate that LPA, but not S1P, is inhibitory to mouse retinal neurites *in vitro*, causing a dose-dependent growth cone collapse and neurite retraction. Furthermore, we have analyzed the response of retinal neurites to LPA from knockout mice for three of the LPA receptor genes (*Lpar1*, *Lpar2*, and *Lpar3*).<sup>8</sup> We demonstrate that the receptors LPA<sub>1</sub>, LPA<sub>2</sub>, and LPA<sub>3</sub> are not required for LPA-induced growth cone collapse and neurite retraction in mouse retinal culture, indicating that one or more other receptors have functional roles in the developing mouse visual system.

## Materials and methods

### Animals and materials

Mice were bred and housed at The Scripps Research Institute (La Jolla, CA, USA) under approved institutional animal care and use committee (IACUC) protocols. For genotyping of tissue, either tail or paw tissue from embryos was removed prior

to retinal isolation and polymerase chain reaction (PCR) was performed as described.<sup>44–46</sup> LPA (18:1 Lyso PA; 1-Oleoyl-2-Hydroxy-sn-Glycero-3-Phosphate) was obtained from Avanti Polar Lipids (Alabaster, AL, USA). LPA was prepared by resuspension in methanol, aliquoting, then evaporating the methanol in a Speed-Vac<sup>®</sup> and storing aliquots at –20°C until use. For use, an aliquot was resuspended in water, then diluted in PBS containing 10% fatty acid-free bovine serum albumin ([BSA] (Sigma, St. Louis, MO, USA), and further diluted in culture media. Sphingosine 1-phosphate (S1P) was obtained from Biomol (Plymouth Meeting, PA) and resuspended in methanol and stored in aliquots at –20°C until use. For use, the required amount was removed and diluted in phosphate buffered saline (PBS) containing 10% fatty acid-free BSA, then further diluted in culture media. Concentrations of S1P higher than 1  $\mu$ M were not tested because of a nonspecific, methanol solvent-induced growth cone collapse that precluded analysis. Ham's F12 media was obtained from Hyclone (Waltham, MA). N2 was obtained from Invitrogen Corporation (Carlsbad, CA); the growth factors brain-derived neurotrophic factor (BDNF) and ciliary neurotrophic factor (CNTF) were obtained from PeproTech (Rocky Hill, NJ, USA); insulin was obtained from Sigma (St. Louis, MO, USA).

### Retinal culture

Retinas were removed from E14.5 mouse embryos obtained by Cesarean section, and the retinas cut into explants. Explants were carefully placed into culture dishes such that they were spaced apart for neurite outgrowth with minimal interactions with other explants. Culture dishes were precoated with 0.1 mg/mL Poly-D-lysine and 10  $\mu$ g/mL laminin (Invitrogen Corporation Carlsbad, CA, USA). Cultures were grown overnight in Ham's F12 media containing N2 supplement along with 5  $\mu$ g/mL insulin + 50 ng/mL BDNF + 10 ng/mL CNTF in a humidified 37°C, 5% CO<sub>2</sub> cell culture incubator.

### Growth cone collapse assay

Retinal explants were cultured overnight on Lab-Tek 4-well chambered coverglass dishes (Nunc, Rochester, NY) in 0.6 mL media. For treatment, 0.2 mL media was removed and 0.2 mL of fresh media containing 3 $\times$  the final LPA or S1P concentration was added and the cultures returned to the CO<sub>2</sub> incubator for 30 minutes. For controls, 0.2 mL fresh media containing a similar amount of PBS + 10% fatty acid-free BSA buffer was added. After 30 minutes incubation, the cultures were then fixed by underlying with

4% paraformaldehyde in PBS. Cultures were permeabilized with 0.1% Triton X-100 and stained with TRITC-conjugated phalloidin (Sigma, St. Louis, MO) and examined under fluorescence microscopy with a 40× objective. For quantification of growth cone collapse, we analyzed all the growth cones at the end of neurites from an explant that were growing on laminin substrate (and not on other neurites or cells). Each growth cone analyzed was classified as “growing”, with lamellipodia and/or filopodia, or as “collapsed”, lacking lamellipodia and filopodia, often with retraction fibers visible. Data from multiple explants from multiple experiments were pooled and the percent growth cone collapse calculated; the number of growth cones, explants, and experiments are presented in Supplementary Tables 1 and 2. Statistical analysis was performed using the Fisher’s exact test. Data was graphed and dose response curves were calculated and applied using GraphPad Prism® software (GraphPad Software, Inc. La Jolla, CA, USA).

For pharmacological inhibition of rho, retinal explants were treated with 5 µg/mL recombinant C3 transferase (Cytoskeleton, Inc. Denver, CO, USA) in media for 20 hours prior to treatment with control media or 100 nM LPA and analyzed for growth cone collapse as described above.

## Time-lapse imaging

Retinal explants were grown overnight in 35 mm coverslip bottom dishes (MatTek, Ashland, MA, USA). For time-lapse imaging, culture dishes were placed on an inverted microscope (Olympus, Center Valley, PA, USA) in a 37°C temperature controlled incubation chamber and humidified CO<sub>2</sub> was passed over the culture dish to maintain pH. Differential interference contrast (DIC) images were collected through a 20× objective every 30 seconds using Metamorph® software (Molecular Devices Downingtown, PA, USA). Growth cones were imaged for 30–40 minutes before any additions were made in order to confirm an active growth state. Subsequently, 1/10 volume of control media was added and cultures imaged for another 15–30 minutes. (Several wild type videos were initially recorded without this control media addition.) Finally, 1/10 volume of media containing 1 µM LPA was added for a final concentration of 100 nM LPA, or 100 nM LPA was added for a final concentration of 10 nM LPA, and imaging continued until no growth cones or neurites were present in the field or until 30 minutes had elapsed. For quantification, the time from LPA addition to the first signs of growth cone collapse was determined. We analyzed a total of 38 growth cones from 18 different explants from wild type embryos, each in its own dish, from

12 animals and 11 different experiments. The resulting data were pooled. In addition, from *Lpar1 Lpar2* mutant embryos, we analyzed an additional 12 growth cones from 6 different explants, each in a different dish, from 3 different mutant embryos over 2 different experiments. Statistical analysis was done using the unpaired t-Test on GraphPad software’s statistical calculator. Videos were produced using Adobe Premiere software.

## Neurite retraction assay

Retinal explants growing in 35 mm coverslip bottom dishes (MatTek, Ashland, MA, USA) were imaged by a panel collection of a 3 × 3 or 4 × 4 box around the explant under a 10 × phase objective to image all the neurites. All panels were then stitched together using Metamorph. Each explant was imaged before treatment and then media containing LPA was added (1/10 volume of media containing LPA at 10 × the final concentration). Each dish was incubated for 30 minutes at 37°C in a 5% CO<sub>2</sub> incubator, and then each explant was imaged again as above. Thresholds were determined in Metamorph to highlight phase-dense objects; neurites were then selected as long and thin objects by Metamorph and subsequently confirmed by observation with manual addition or removal. The total area of phase-dense neurites was calculated by Metamorph, which we used as total neurite length, both before and after treatment. Percent neurite retraction was calculated from total neurite lengths as “((before-after)/before × 100).” The total number of explants and animals examined is presented in Supplementary Table 3. Statistical analysis was done by one-way ANOVA with Tukey’s post hoc test (set at  $P < 0.05$ ) via GraphPad Prism software.

## Results

LPA has been shown to be inhibitory for neurite growth, eliciting neurite retraction in vitro in a variety of primary neurons and neural cell lines.<sup>16–27</sup> As a first step in our investigation, we characterized the responses of embryonic mouse retinal neurites to LPA in vitro. LPA caused a rapid growth cone collapse in E14.5 mouse retinal neurites in culture grown on laminin as evidenced by loss of growth cone lamellipodia and filopodia (Figure 1). This LPA-mediated growth cone collapse was rapid, usually occurring within 5 minutes (see Table 1), and was followed by neurite retraction (see Figure 4 and video in Supplementary Figure S1). A growth cone collapse assay was used to quantify the responses to LPA exposure. All isolated retinal growth cones (those not growing on other neurites, growth cones, or soma) were

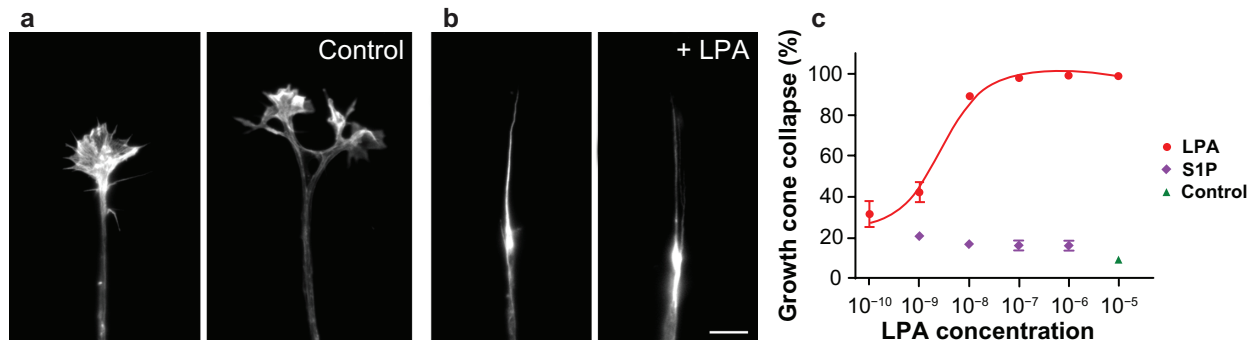


**Figure 1** Collapse of mouse retinal growth cones after treatment with LPA. Fluorescent images of F-actin stained with TRITC-Phalloidin from two examples of growth cones under control conditions (a) or two examples of collapsed retinal growth cones after treatment with 100 nM LPA for 30 minutes (b). Note abundant lamellipodia and filopodia under control conditions (a) which are absent in collapsed growth cones treated with LPA (b). Scale bar: 10  $\mu$ m. (c) Graph of quantification of growth cone collapse (100% indicating all growth cones collapsed) assayed after 30 minutes of treatment with various concentrations (log scale, molar) of LPA ( $\bullet$ ) shows a dose-dependent response compared to control ( $\blacktriangle$ ) or S1P treatment ( $\blacklozenge$ ). Data from multiple explants of multiple experiments (see Supplementary Table 1); bars show SEM.

**Abbreviations:** LPA, lysophosphatidic acid; SEM, standard error of mean.

examined and classified as having normal morphology or collapsed morphology after treatment with media containing various concentrations of LPA (or control media). This quantitative growth cone collapse assay showed that the response to LPA was dose-dependent (Figure 1c). Under control conditions, about 10%–20% of mouse retinal growth cones showed a collapsed morphology. Upon treatment with LPA, we observed complete growth cone collapse with LPA concentrations of 100 nanomolar or greater and a half maximal response in the 2–5 nanomolar range. Furthermore, this response was specific in that another lysophospholipid, sphingosine 1-phosphate (S1P), did not elicit mouse retinal growth cone collapse, even at micromolar concentrations (Figure 1c).

To further verify that this LPA response is a specific growth cone response, we analyzed LPA receptor activated intracellular signaling. In neuronal cell lines, LPA-induced growth cone collapse and/or neurite retraction has been demonstrated to signal through the rho pathway.<sup>19,20,25,47</sup> Thus, we blocked the rho pathway by treatment with C3 transferase, which ADP ribosylates rho and inactivates it. Treatment

of retinal explants with C3 transferase greatly reduced the growth cone collapse produced by 100 nM LPA: 23% growth cone collapse with C3 treatment compared to 94% growth cone collapse without C3 (both with 100 nM LPA;  $P < 0.0001$ ). Thus, the LPA-induced growth cone collapse of mouse retinal neurites requires intracellular signaling via the rho pathway.

We assessed the role of the LPA receptors LPA<sub>1</sub>, LPA<sub>2</sub>, and LPA<sub>3</sub> on retinal neurons through mutant mice homozygous for targeted deletions in *Lpar1*, *Lpar2*, and *Lpar3*. These mice have been characterized previously as functional nulls.<sup>44,46,48</sup> We used the growth cone collapse assay to analyze the effects of LPA on retinal tissue isolated from homozygous mutant embryos for these LPA receptors, either singly (for *Lpar2*) or in combinations of double or triple mutants. No difference was seen in the amount of neurite outgrowth (data not shown) or growth cone morphology (Figures 2a–c for example with *Lpar2* mutant) between wild type and mutant retinal cultures under control conditions; the growth cones from retinas of mutant mice showed normal lamellipodial and filopodial morphology. In addition, the percentage of growth cones showing a collapsed morphology under control conditions was about 10% in all LPA receptor mutants examined, similar to wild type controls (see Figure 3). Upon treatment with LPA, growth cone collapse was still observed in retinal cultures from *Lpar2* mutants (Figures 2f–h) as well as double and triple mutants (Figure 3). These collapsed growth cones, observed after LPA addition in the mutant mouse cultures, were indistinguishable from those seen from wild type mice (Figures 2d–e). To further characterize the responses in mutant cultures, we quantified the growth cone collapse response to LPA concentrations from 1 nM to

**Table 1** Dynamic growth cone properties

	Sample size (n)	Median time to collapse
Wild type	38	2 minutes
<i>Lpar1 Lpar2</i>	12	1 minutes

**Notes:** Analysis of time-lapse imaging of LPA treatment of retinal neurites from wild type and *Lpar1 Lpar2* double mutant mice. Sample size (number of growth cones analyzed) and median time to growth cone collapse after LPA treatment are shown. There is no statistical difference in time to growth cone collapse ( $P = 0.23$ ).

**Abbreviation:** LPA, lysophosphatidic acid.

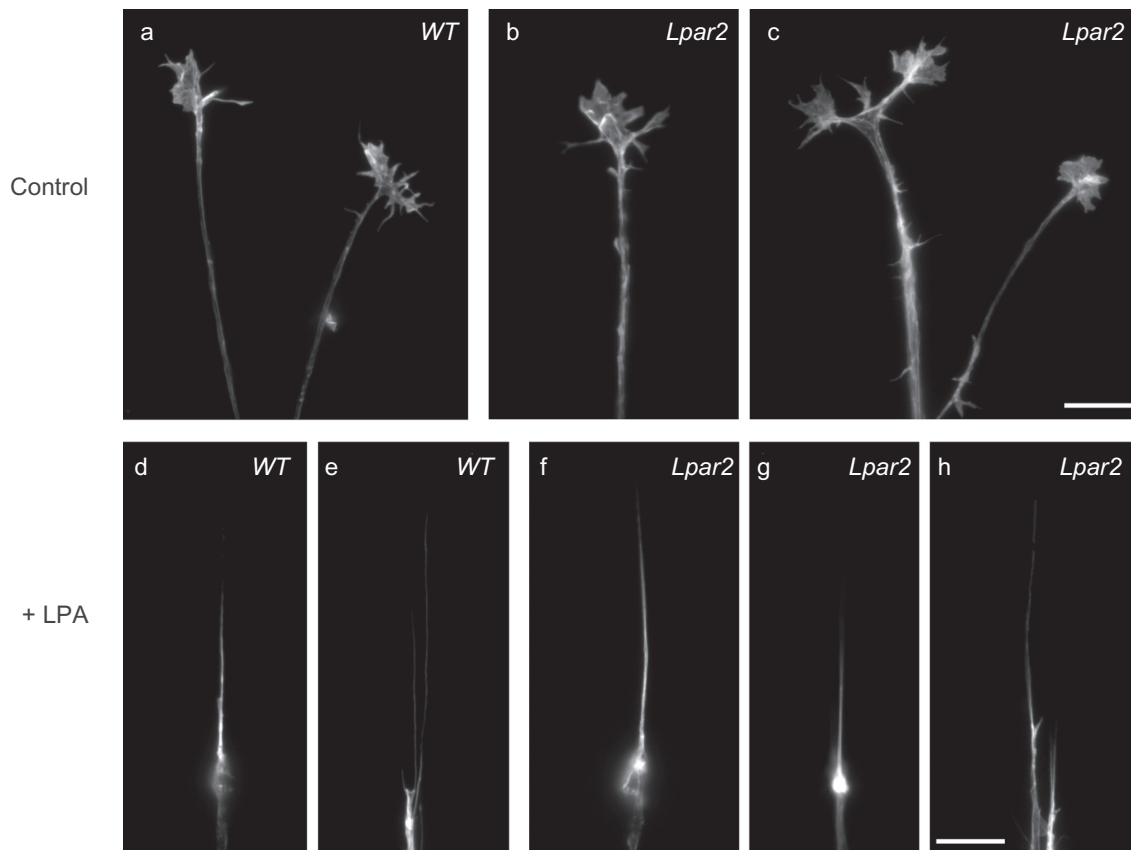


**Figure 2** LPA-induced growth cone collapse in *Lpar2* mutant retina neurites. Growth cones from E14.5 retinal neurites under control conditions (a–c) or after treatment with 100 nM LPA for 30 minutes (d–h) stained with TRITC-Phalloidin. Retinal growth cones from *Lpar2* mutant embryos (b–c, f–h) show similar morphology to wild type littermates (a, d–e), both under control conditions (a–c) and after LPA treatment (d–h). Similar growth cone collapse is seen in the *Lpar2* mutant retina as in wild type. Scale bars: 15  $\mu$ m.

**Abbreviation:** LPA, lysophosphatidic acid.

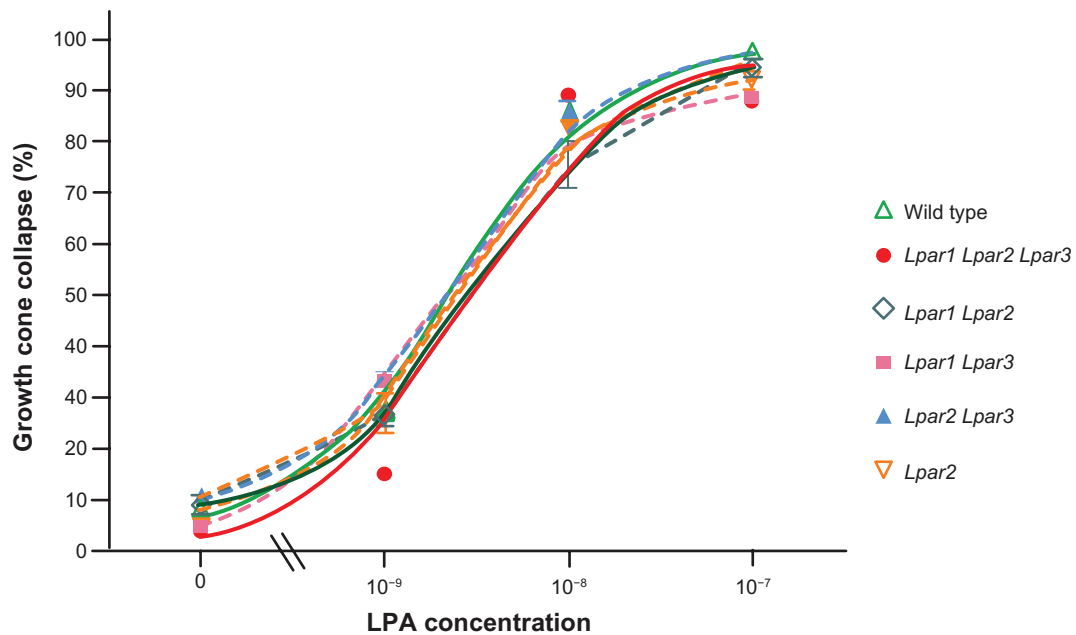


**Figure 3** Quantification of growth cone collapse of retinal neurites from LPA receptor mutants. Percentage of growth cones showing collapsed morphology from observations of retinal explants of various mouse LPA receptor genotypes under control conditions (0 LPA) or 1 nM, 10 nM, or 100 nM LPA concentrations (log scale, molar). Each data point is from multiple explants collected from multiple animals (see Supplementary Table 2), with bars representing SEM from different animals. Wild type data are from littermates.

**Abbreviations:** LPA, lysophosphatidic acid; SEM, standard error of mean.

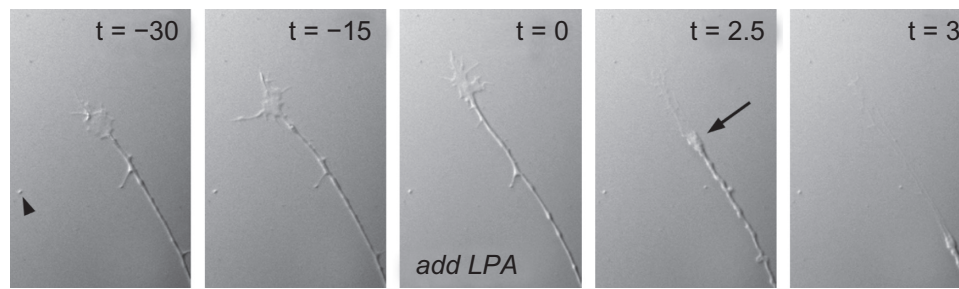


**Figure 4** Time-lapse images of retinal growth cone response to LPA. DIC images from time-lapse recordings of a retinal growth cone growing in culture on laminin. Sequence of images show growth from 30 minutes prior to LPA treatment ( $t = -30$ ) to time of addition of LPA ( $t = 0$ ). Subsequently, 2.5 minutes after LPA addition ( $t = 2.5$ ), the growth cone has begun to collapse (arrow), and by 3 minutes after LPA addition ( $t = 3$ ), the growth cone has completely collapsed and the neurite is retracting. A small piece of debris (arrowhead) is indicated for reference. Time in minutes is designated relative to time of LPA addition ( $t = 0$ ).

**Abbreviations:** LPA, lysophosphatidic acid; SEM, standard error of mean; t, time; DIC, differential interference contrast.

100 nM. Surprisingly, a significant dose-dependent growth cone collapse response to LPA was seen in all mutant retinal tissue examined (Figure 3). Even retinal tissue from mice with homozygous deletions of all three receptor genes (*Lpar1*, *Lpar2*, and *Lpar3*) showed a dose-dependent retinal growth cone collapse response that approached complete collapse at 100 nM LPA and which showed significant growth cone collapse at 1 nM LPA compared to control ( $P < 0.001$ ). Interestingly, the *Lpar1 Lpar2 Lpar3* triple-null mutant retinal tissue does show a statistically significant lower growth cone collapse response at 1 nM LPA compared to wild type or any of the other double mutant combinations ( $P < 0.01$  for each pairwise analysis). Thus, loss of these three LPA receptors partially, but not completely, reduced the most sensitive LPA-induced growth cone collapse. Nonetheless, since significant growth cone collapse is still found, the receptors LPA<sub>1</sub>, LPA<sub>2</sub>, and LPA<sub>3</sub> are not required for LPA-mediated growth cone collapse of mouse retinal neurites.

We observed very little difference in our retinal growth cone collapse assay upon LPA treatment in mice lacking receptors LPA<sub>1-3</sub> compared to wild type mice. However, as the growth cone collapse assay is a static assay, we also examined the dynamic responses of retinal growth cones to LPA through time-lapse imaging. Retinal growth cones from wild type mice showed a rapid collapse upon treatment with LPA (see Figure 4 and Supplementary Figure S1 together with Table 1), but no responses were observed in the same growth cones upon addition of control media. Similar to wild type, retinal growth cones from *Lpar1 Lpar2* double mutant mice also responded to LPA with rapid growth cone collapse (Table 1). (As LPA<sub>3</sub> has not been demonstrated to signal through the  $G\alpha_{12/13}$  rho pathway which is suggested to mediate growth cone collapse,<sup>40,49,50</sup> the *Lpar3* mutant mouse was not analyzed here.) Analysis of response time to LPA addition showed no significant difference ( $P = 0.23$ )

between wild type and *Lpar1 Lpar2* double mutant mice in time to collapse (Table 1); the median response times were quite similar, in the range of 1–2 minutes. In addition, examination of the morphology of the *Lpar1 Lpar2* mutant growth cones under control conditions, or after LPA treatment, was indistinguishable from the morphologies seen from wild type growth cones (data not shown). Thus, by analysis of dynamic responses of retinal growth cones, no difference was observed in response to LPA after the loss of the LPA receptors LPA<sub>1</sub> and LPA<sub>2</sub>.

In addition to growth cone collapse, LPA induces neurite retraction. As the receptors LPA<sub>1</sub>, LPA<sub>2</sub>, and LPA<sub>3</sub> are not required for growth cone collapse, we also investigated whether they may be required for neurite retraction. We examined neurite retraction by measuring the change in total neurite length after treatment with LPA. Because the retinal explants were not uniform, and thus neurite outgrowth was variable, as was neurite fasciculation, we measured neurite retraction by imaging and quantifying from the same explants both before and after treatment with LPA. In retinal explants from wild type embryos, there was considerable neurite retraction upon treatment with LPA (Figures 5a–b). We quantified this loss of neurites by percent neurite retraction. Control media addition showed no neurite retraction; indeed, a “negative retraction” was often observed because of neurite growth. However, treatment with LPA produced a dose-dependent neurite retraction (Figure 6a) that was statistically significant ( $P < 0.01$  versus control and other concentrations). We then examined the neurites of retinal explants from homozygous LPA receptor mutant mice focusing on the 10 nM LPA concentration where LPA-induced neurite retraction was high but not saturating (Figure 6b). Before LPA treatment, retinal explants from LPA receptor mutants, including triple mutants, had similar levels of neurite outgrowth, as well as similar variability of neurite

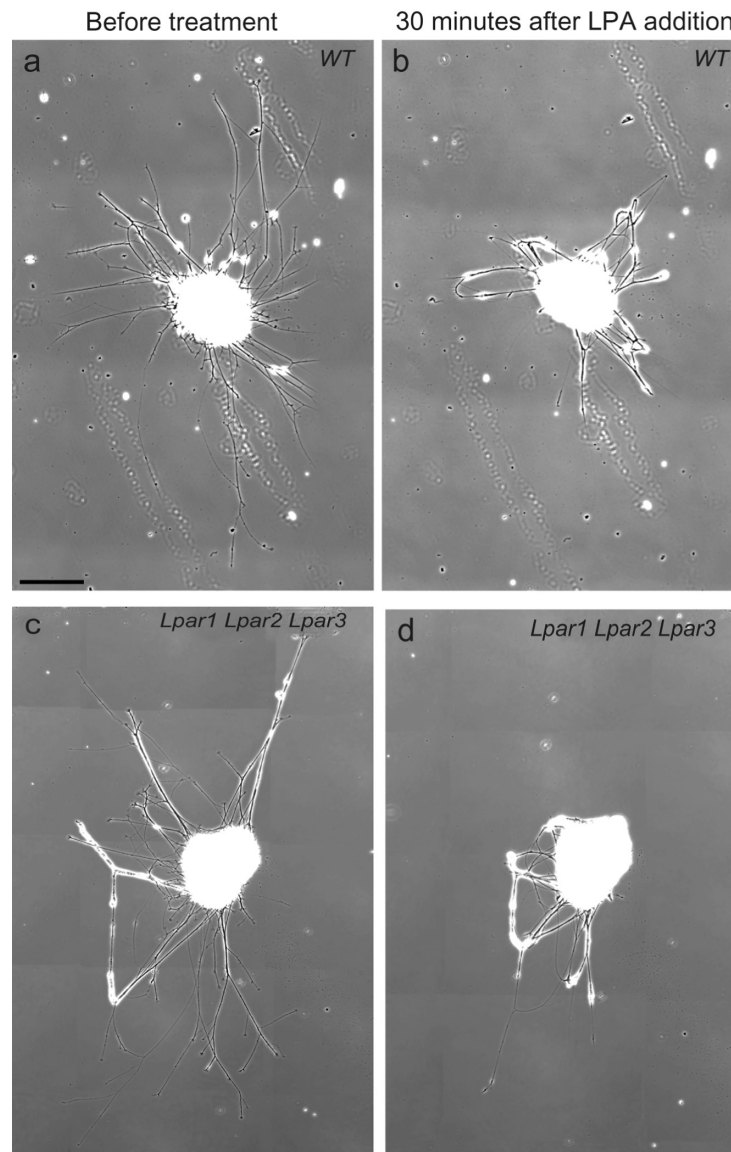


**Figure 5** Neurite retraction after LPA treatment. Phase contrast image montages of retinal explants and neurites from wild type E14.5 mouse embryos (a–b) and *Lpar1 Lpar2 Lpar3* triple mutant embryos (c–d). The same explants were imaged before (a, c) and after (b, d) LPA treatment for 30 minutes, showing dramatic neurite retraction. Scale bars: 200  $\mu$ m.

**Abbreviation:** LPA, lysophosphatidic acid.

fasciculation, as wild type (data not shown). Neurite retraction was observed with LPA treatment of retinal explants from LPA receptor mutants, including triple mutants homozygous for deletion of *Lpar1 Lpar2 Lpar3* (Figures 5c–d). This neurite retraction was quantified (Figure 6b) and was clearly observed at 10 nM LPA in triple, as well as double and single LPA receptor mutants. There was no statistically significant neurite retraction difference between wild type and the mutants with 10 nM LPA treatment of retinal explants (ANOVA with Tukey's post hoc test). In addition, analysis of a small number of *Lpar1 Lpar2 Lpar3* triple mutant retinas showed almost complete neurite retraction

(mean = 94%) at 100 nM LPA (data not shown). Thus, our data demonstrate that the LPA receptors LPA<sub>1</sub>, LPA<sub>2</sub>, and LPA<sub>3</sub> are not required for neurite retraction.

## Discussion

LPA is an extracellular signaling molecule that has previously been shown to have inhibitory effects on process outgrowth in a variety of neural cell lines as well as in primary neurons.<sup>16–27</sup> We have confirmed this inhibitory effect in primary mouse retinal neurons by showing that LPA can cause both growth cone collapse and neurite retraction. This effect is potent, with effects demonstrable in the nanomolar range, and

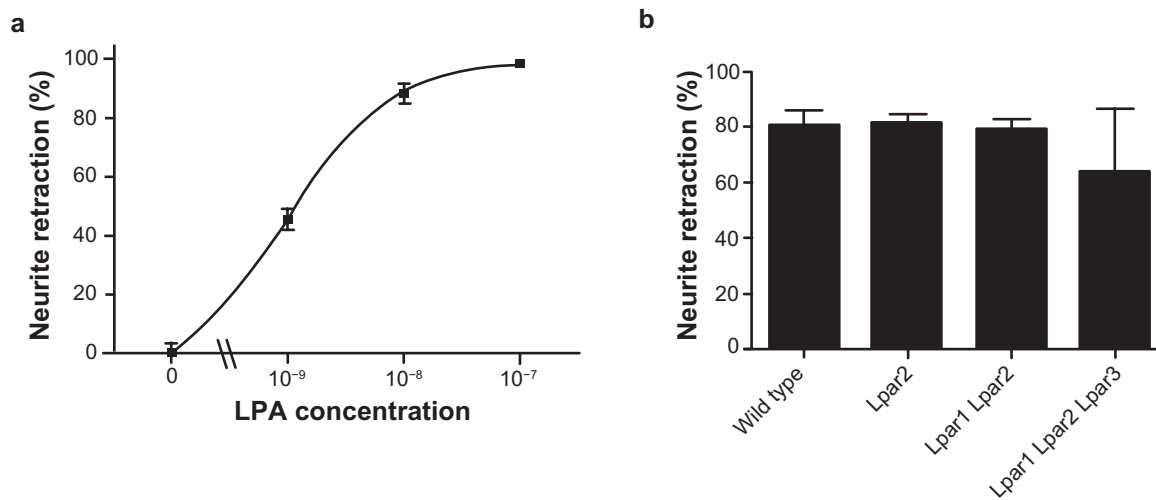


**Figure 6** Quantification of neurite retraction. Neurite retraction from wild type mouse retinal explants shows a dose-dependent response to LPA (a). Neurite retraction is measured as percent of total neurite length lost per explant after 30 minute incubation with 1 nM, 10 nM, or 100 nM LPA (log scale, molar) or control media (0) compared to total neurite length before treatment. 100% indicates complete loss of neurites, 0% retraction indicates no net change, and negative values indicate growth. Neurite retraction was observed in retinal explants from LPA receptor mutants after treatment with 10 nM LPA for 30 minutes (b). No significant differences in neurite retraction levels were observed between mutant and wild type retinal explants (ANOVA). Data presented from multiple explants of multiple experiments (see Supplementary Table 3); bars show SEM.

**Abbreviations:** LPA, lysophosphatidic acid; ANOVA, analysis of variation; SEM, standard error of mean.

functions through the rho pathway. Furthermore, the growth cone collapse response and initiation of neurite retraction is rapid, usually occurring in less than 5 minutes.

LPA signals through several GPCRs, of which five have been clearly shown to be activated by LPA. The first three of these to be identified, now called LPA<sub>1</sub>, LPA<sub>2</sub>, and LPA<sub>3</sub>, form a family of homologous receptors.<sup>30,38,40,46</sup> Primary mouse retinal neurons do not require these LPA receptors for growth cone collapse or neurite retraction. LPA was shown to have potent effects even in retinal neurites from mice simultaneously lacking LPA<sub>1</sub>, LPA<sub>2</sub>, and LPA<sub>3</sub>, indicating that these receptors are not required. Although LPA<sub>1</sub>, LPA<sub>2</sub>, and LPA<sub>3</sub> are not required, they still may function to induce growth cone collapse and neurite retraction in retinal neurites. This function is indicated by the small but significant reduction in growth cone collapse at 1 nM LPA observed in the *Lpar1 Lpar2 Lpar3* triple mutant retinal neurites. However, this function is not required and is likely to be redundant to one or more other LPA receptors that could rescue their absence.

If the receptors LPA<sub>1</sub>, LPA<sub>2</sub>, and LPA<sub>3</sub> are not required, what receptor does mediate LPA-induced growth cone collapse and neurite retraction in mouse retinal neurons? Recently, two new GPCRs have been identified, named LPA<sub>4</sub> and LPA<sub>5</sub>,<sup>34-36,41,51</sup> with there still being other possible receptors that require further validation.<sup>8,52,53</sup> Any one of these actual or putative receptors may mediate LPA-induced growth cone collapse and neurite retraction in mouse retinal neurites. Further analyses of mice lacking *Lpar4* or *Lpar5* in a background of

*Lpar1 Lpar2 Lpar3* deficiency could clarify this; however such mutants do not currently exist. It is also possible that unknown receptor(s) could mediate these responses.

In addition to the potency of LPA for mouse retinal growth cone collapse, we examined the specificity of LPA compared to the related lysophospholipid S1P. In mouse retinal cultures, S1P did not induce growth cone collapse at concentrations up to 1 μM, indicating that the growth cone collapse response to LPA was not due to nonspecific lysophospholipid effects. In previous reports, S1P did produce cell rounding in N1E115 neuroblastoma cells<sup>21</sup> and PC12 cells.<sup>23</sup> Furthermore, Strohlic and colleagues<sup>24</sup> recently reported that in *Xenopus* retinal cells, S1P did induce growth cone collapse and a negative turning response. However, Toman and colleagues<sup>54</sup> found that in both PC12 and dorsal root ganglia (DRG) neurons, S1P led to neurite extension in established cultures, although it was inhibitory in freshly dissociated DRG cultures. Thus, the role of S1P on neurite growth is variable depending on the species and culture system. In embryonic mouse retinal cultures, S1P does not appear to be inhibitory.

The *in vivo* role of this LPA-mediated inhibitory effect on axons is not known. Many established axon guidance cues cause growth cone collapse *in vitro* and are inhibitory cues *in vivo*.<sup>55-65</sup> LPA is found in the central nervous system,<sup>66,67</sup> as well as other tissues,<sup>66</sup> and thus has the potential of acting as an *in vivo* axon guidance cue. Enzymes responsible for LPA production, particularly autotaxin, are also found in



the central nervous system,<sup>68–72</sup> and at least one isoform of autotaxin appears to be enriched in the CNS.<sup>71,73,74</sup> Interestingly, recent evidence suggests that S1P may be an axon guidance cue for retinal axons to innervate the tectum in the *Xenopus* visual system,<sup>24</sup> indicating that lysophospholipids could be axon guidance cues. Furthermore, CNS expression of up to five distinct receptors for both LPA and S1P may underscore additional functions and complex roles during development, which await further study.

## Acknowledgements

We thank Danielle Letourneau for editorial assistance, Kyoko Noguchi for comments on the manuscript, and the NIH (MH051699, NS048478, and DA019674 to J.C.) for support of this work.

## Disclosures

The authors have no conflicts of interest that are directly relevant to the content of this study.

## References

1. Goodman CS, Shatz CJ. Developmental mechanisms that generate precise patterns of neuronal connectivity. *Cell*. 1993;72(Suppl):77–98.
2. McLaughlin T, O'Leary DD. Molecular gradients and development of retinotopic maps. *Annu Rev Neurosci*. 2005;28:327–355.
3. Schmitt AM, Shi J, Wolf AM, Lu CC, King LA, Zou Y. Wnt-Ryk signalling mediates medial-lateral retinotectal topographic mapping. *Nature*. 2006;439(7072):31–37.
4. Simon DK, O'Leary DD. Responses of retinal axons in vivo and in vitro to position-encoding molecules in the embryonic superior colliculus. *Neuron*. 1992;9(5):977–989.
5. Lemke G, Reber M. Retinotectal mapping: new insights from molecular genetics. *Annu Rev Cell Dev Biol*. 2005;21:551–580.
6. Herr DR, Chun J. Effects of LPA and S1P on the nervous system and implications for their involvement in disease. *Curr Drug Targets*. 2007;8(1):155–167.
7. Rivera R, Chun J. Biological effects of lysophospholipids. *Rev Physiol Biochem Pharmacol*. 2008;160:25–46.
8. Choi JW, Herr DR, Noguchi K, et al. LPA Receptors: Subtypes and Biological Actions. *Annu Rev Pharmacol Toxicol*. 2010;50(1). In press.
9. Anliker B, Chun J. Lysophospholipid G protein-coupled receptors. *J Biol Chem*. 2004;279(20):20555–20558.
10. Ishii I, Fukushima N, Ye X, Chun J. Lysophospholipid receptors: signaling and biology. *Annu Rev Biochem*. 2004;73:321–354.
11. Moolenaar WH, van Meeteren LA, Giepmans BN. The ins and outs of lysophosphatidic acid signaling. *Bioessays*. 2004;26(8):870–881.
12. Birgbauer E, Chun J. New developments in the biological functions of lysophospholipids. *Cell Mol Life Sci*. 2006;63(23):2695–2701.
13. Kingsbury MA, Rehen SK, Contos JJ, Higgins CM, Chun J. Non-proliferative effects of lysophosphatidic acid enhance cortical growth and folding. *Nat Neurosci*. 2003;6(12):1292–1299.
14. Inoue M, Rashid MH, Fujita R, Contos JJ, Chun J, Ueda H. Initiation of neuropathic pain requires lysophosphatidic acid receptor signaling. *Nat Med*. 2004;10(7):712–718.
15. Trimbuch T, Beed P, Vogt J, et al. Synaptic PRG-1 Modulates Excitatory Transmission via Lipid Phosphate-Mediated Signaling. *Cell*. 2009;138(6):1222–1235.
16. Campbell DS, Holt CE. Chemotropic responses of retinal growth cones mediated by rapid local protein synthesis and degradation. *Neuron*. 2001;32(6):1013–1026.
17. Hirose M, Ishizaki T, Watanabe N, et al. Molecular dissection of the Rho-associated protein kinase (p160ROCK)-regulated neurite remodeling in neuroblastoma N1E-115 cells. *J Cell Biol*. 1998;141(7):1625–1636.
18. Jalink K, Eichholtz T, Postma FR, van Corven EJ, Moolenaar WH. Lysophosphatidic acid induces neuronal shape changes via a novel, receptor-mediated signaling pathway: similarity to thrombin action. *Cell Growth Differ*. 1993;4(4):247–255.
19. Jalink K, van Corven EJ, Hengeveld T, Morii N, Narumiya S, Moolenaar WH. Inhibition of lysophosphatidate- and thrombin-induced neurite retraction and neuronal cell rounding by ADP-ribosylation of the small GTP-binding protein Rho. *J Cell Biol*. 1994;126(3):801–810.
20. Kozma R, Samer S, Ahmed S, Lim L. Rho family GTPases and neuronal growth cone remodelling: relationship between increased complexity induced by Cdc42Hs, Rac1, and acetylcholine and collapse induced by RhoA and lysophosphatidic acid. *Mol Cell Biol*. 1997;17(3):1201–1211.
21. Postma FR, Jalink K, Hengeveld T, Moolenaar WH. Sphingosine-1-phosphate rapidly induces Rho-dependent neurite retraction: action through a specific cell surface receptor. *Embo J*. 1996;15(10):2388–2392.
22. Saito S. Effects of lysophosphatidic acid on primary cultured chick neurons. *Neurosci Lett*. 1997;229(2):73–76.
23. Sato K, Tomura H, Igarashi Y, Ui M, Okajima F. Exogenous sphingosine 1-phosphate induces neurite retraction possibly through a cell surface receptor in PC12 cells. *Biochem Biophys Res Commun*. 1997;240(2):329–334.
24. Strohlic L, Dwivedy A, van Horck FP, Falk J, Holt CE. A role for S1P signalling in axon guidance in the *Xenopus* visual system. *Development*. 2008;135(2):333–342.
25. Tigyi G, Fischer DJ, Sebok A, Marshall F, Dyer DL, Miledi R. Lysophosphatidic acid-induced neurite retraction in PC12 cells: neurite-protective effects of cyclic AMP signaling. *J Neurochem*. 1996;66(2):549–558.
26. Tigyi G, Fischer DJ, Sebok A, Yang C, Dyer DL, Miledi R. Lysophosphatidic acid-induced neurite retraction in PC12 cells: control by phosphoinositide-Ca<sup>2+</sup> signaling and Rho. *J Neurochem*. 1996;66(2):537–548.
27. Zhang XF, Schaefer AW, Burnette DT, Schoonderwoert VT, Forscher P. Rho-dependent contractile responses in the neuronal growth cone are independent of classical peripheral retrograde actin flow. *Neuron*. 2003;40(5):931–944.
28. Hecht JH, Weiner JA, Post SR, Chun J. Ventricular zone gene-1 (vzq-1) encodes a lysophosphatidic acid receptor expressed in neurogenic regions of the developing cerebral cortex. *J Cell Biol*. 1996;135(4):1071–1083.
29. Hla T, Maciag T. An abundant transcript induced in differentiating human endothelial cells encodes a polypeptide with structural similarities to G-protein-coupled receptors. *J Biol Chem*. 1990;265(16):9308–9313.
30. Chun J, Goetzl EJ, Hla T, et al. International Union of Pharmacology. XXXIV. Lysophospholipid receptor nomenclature. *Pharmacol Rev*. 2002;54(2):265–269.
31. Kluk MJ, Hla T. Signaling of sphingosine-1-phosphate via the S1P/EDG-family of G-protein-coupled receptors. *Biochim Biophys Acta*. 2002;1582(1–3):72–80.
32. Lagerstrom MC, Schioth HB. Structural diversity of G protein-coupled receptors and significance for drug discovery. *Nat Rev Drug Discov*. 2008;7(4):339–357.
33. Siehler S. Cell-based assays in GPCR drug discovery. *Biotechnol J*. 2008;3(4):471–483.
34. Noguchi K, Ishii S, Shimizu T. Identification of p2y9/GPR23 as a novel G protein-coupled receptor for lysophosphatidic acid, structurally distant from the Edg family. *J Biol Chem*. 2003;278(28):25600–25606.

35. Kotarsky K, Boketoft A, Bristulf J, et al. Lysophosphatidic acid binds to and activates GPR92, a G protein-coupled receptor highly expressed in gastrointestinal lymphocytes. *J Pharmacol Exp Ther.* 2006;318(2):619–628.
36. Lee CW, Rivera R, Gardell S, Dubin AE, Chun J. GPR92 as a new G<sub>12/13</sub>- and G<sub>q</sub>-coupled lysophosphatidic acid receptor that increases cAMP, LPA<sub>3</sub>. *J Biol Chem.* 2006;281(33):23589–23597.
37. An S, Bleu T, Hallmark OG, Goetzl EJ. Characterization of a novel subtype of human G protein-coupled receptor for lysophosphatidic acid. *J Biol Chem.* 1998;273(14):7906–7910.
38. Bandoh K, Aoki J, Hosono H, et al. Molecular cloning and characterization of a novel human G-protein-coupled receptor, EDG7, for lysophosphatidic acid. *J Biol Chem.* 1999;274(39):27776–27785.
39. Contos JJ, Ishii I, Chun J. Lysophosphatidic acid receptors. *Mol Pharmacol.* 2000;58(6):1188–1196.
40. Ishii I, Contos JJ, Fukushima N, Chun J. Functional comparisons of the lysophosphatidic acid receptors, LP(A1)/VZG-1/EDG-2, LP(A2)/EDG-4, and LP(A3)/EDG-7 in neuronal cell lines using a retrovirus expression system. *Mol Pharmacol.* 2000;58(5):895–902.
41. Lee CW, Rivera R, Dubin AE, Chun J. LPA(4)/GPR23 is a lysophosphatidic acid (LPA) receptor utilizing G(s)-, G(q)/G(i)-mediated calcium signaling and G(12/13)-mediated Rho activation. *J Biol Chem.* 2007;282(7):4310–4317.
42. Fukushima N, Kimura Y, Chun J. A single receptor encoded by vzg-1/lpa1/edg-2 couples to G proteins and mediates multiple cellular responses to lysophosphatidic acid. *Proc Natl Acad Sci U S A.* 1998;95(11):6151–6156.
43. Erskine L, Herrera E. The retinal ganglion cell axon's journey: insights into molecular mechanisms of axon guidance. *Dev Biol.* 2007;308(1):1–14.
44. Contos JJ, Fukushima N, Weiner JA, Kaushal D, Chun J. Requirement for the lpa1 lysophosphatidic acid receptor gene in normal suckling behavior. *Proc Natl Acad Sci U S A.* 2000;97(24):13384–13389.
45. Contos JJ, Chun J. The mouse lp(A3)/Edg7 lysophosphatidic acid receptor gene: genomic structure, chromosomal localization, and expression pattern. *Gene.* 2001;267(2):243–253.
46. Contos JJ, Ishii I, Fukushima N, et al. Characterization of lpa(2) (Edg4) and lpa(1)/lpa(2) (Edg2/Edg4) lysophosphatidic acid receptor knock-out mice: signaling deficits without obvious phenotypic abnormality attributable to lpa(2). *Mol Cell Biol.* 2002;22(19):6921–6929.
47. Fukushima N, Ishii I, Habara Y, Allen CB, Chun J. Dual regulation of actin rearrangement through lysophosphatidic acid receptor in neuroblast cell lines: actin depolymerization by Ca(2+)-alpha-actinin and polymerization by rho. *Mol Biol Cell.* 2002;13(8):2692–2705.
48. Ye X, Hama K, Contos JJ, et al. LPA3-mediated lysophosphatidic acid signalling in embryo implantation and spacing. *Nature.* 2005;435(7038):104–108.
49. Kranenburg O, Poland M, van Horck FP, Drechsel D, Hall A, Moolenaar WH. Activation of RhoA by lysophosphatidic acid and Galpha12/13 subunits in neuronal cells: induction of neurite retraction. *Mol Biol Cell.* 1999;10(6):1851–1857.
50. Bito H, Furuyashiki T, Ishihara H, et al. A critical role for a Rho-associated kinase, p160ROCK, in determining axon outgrowth in mammalian CNS neurons. *Neuron.* 2000;26(2):431–441.
51. Yanagida K, Ishii S, Hamano F, Noguchi K, Shimizu T. LPA4/p2y9/GPR23 mediates rho-dependent morphological changes in a rat neuronal cell line. *J Biol Chem.* 2007;282(8):5814–5824.
52. Pasternack SM, von Kugelgen I, Aboud KA, et al. G protein-coupled receptor P2Y5 and its ligand LPA are involved in maintenance of human hair growth. *Nat Genet.* 2008;40(3):329–334.
53. Yanagida K, Masago K, Nakanishi H, et al. Identification and characterization of a novel lysophosphatidic acid receptor, p2y5/LPA6. *J Biol Chem.* 2009;284(26):17731–17741.
54. Toman RE, Payne SG, Watterson KR, et al. Differential transactivation of sphingosine-1-phosphate receptors modulates NGF-induced neurite extension. *J Cell Biol.* 2004;166(3):381–392.
55. Cox EC, Muller B, Bonhoeffer F. Axonal guidance in the chick visual system: posterior tectal membranes induce collapse of growth cones from the temporal retina. *Neuron.* 1990;4(1):31–37.
56. Drescher U, Kremoser C, Handwerker C, Loschinger J, Noda M, Bonhoeffer F. In vitro guidance of retinal ganglion cell axons by RAGS, a 25 kDa tectal protein related to ligands for Eph receptor tyrosine kinases. *Cell.* 1995;82(3):359–370.
57. Frisén J, Yates PA, McLaughlin T, Friedman GC, O'Leary DDM, Barbacid M. Ephrin-A5 (AL-1/RAGS) is essential for proper retinal axon guidance and topographic mapping in the mammalian visual system. *Neuron.* 1998;20(2):235–243.
58. Feldheim DA, Kim YI, Bergemann AD, Frisen J, Barbacid M, Flanagan JG. Genetic analysis of ephrin-A2 and ephrin-A5 shows their requirement in multiple aspects of retinocollicular mapping. *Neuron.* 2000;25(3):563–574.
59. Luo Y, Raible D, Raper JA. Collapsin: a protein in brain that induces the collapse and paralysis of neuronal growth cones. *Cell.* 1993;75(2):217–227.
60. Behar O, Golden JA, Mashimo H, Schoen FJ, Fishman MC. Semaphorin III is needed for normal patterning and growth of nerves, bones and heart. *Nature.* 1996;383(6600):525–528.
61. Taniguchi M, Yuasa S, Fujisawa H, et al. Disruption of semaphorin III/D gene causes severe abnormality in peripheral nerve projection. *Neuron.* 1997;19(3):519–530.
62. Isbister CM, Tsai A, Wong ST, Kolodkin AL, O'Connor TP. Discrete roles for secreted and transmembrane semaphorins in neuronal growth cone guidance in vivo. *Development.* 1999;126(9):2007–2019.
63. Niclou SP, Jia L, Raper JA. Slit2 is a repellent for retinal ganglion cell axons. *J Neurosci.* 2000;20(13):4962–4974.
64. Bagri A, Marin O, Plump AS, et al. Slit proteins prevent midline crossing and determine the dorsoventral position of major axonal pathways in the mammalian forebrain. *Neuron.* 2002;33(2):233–248.
65. Plump AS, Erskine L, Sabatier C, et al. Slit1 and Slit2 cooperate to prevent premature midline crossing of retinal axons in the mouse visual system. *Neuron.* 2002;33(2):219–232.
66. Das AK, Hajra AK. Quantification, characterization and fatty acid composition of lysophosphatidic acid in different rat tissues. *Lipids.* 1989;24(4):329–333.
67. Sugiura T, Nakane S, Kishimoto S, et al. Occurrence of lysophosphatidic acid and its alkyl ether-linked analog in rat brain and comparison of their biological activities toward cultured neural cells. *Biochim Biophys Acta.* 1999;1440(2–3):194–204.
68. Dennis J, Nogaroli L, Fuss B. Phosphodiesterase-Ialpha/autotaxin (PD-Ialpha/ATX): A multifunctional protein involved in central nervous system development and disease. *J Neurosci Res.* 2005;82(6):737–742.
69. Sato K, Malchinkhuu E, Muraki T, et al. Identification of autotaxin as a neurite retraction-inducing factor of PC12 cells in cerebrospinal fluid and its possible sources. *J Neurochem.* 2005;92(4):904–914.
70. Lee HY, Murata J, Clair T, et al. Cloning, chromosomal localization, and tissue expression of autotaxin from human teratocarcinoma cells. *Biochem Biophys Res Commun.* 1996;218(3):714–719.
71. Giganti A, Rodriguez M, Fould B, et al. Murine and human autotaxin alpha, beta, and gamma isoforms: gene organization, tissue distribution, and biochemical characterization. *J Biol Chem.* 2008;283(12):7776–7789.
72. Ohuchi H, Hayashibara Y, Matsuda H, et al. Diversified expression patterns of autotaxin, a gene for phospholipid-generating enzyme during mouse and chicken development. *Dev Dyn.* 2007;236(4):1134–1143.
73. Narita M, Goji J, Nakamura H, Sano K. Molecular cloning, expression, and localization of a brain-specific phosphodiesterase I/nucleotide pyrophosphatase (PD-I alpha) from rat brain. *J Biol Chem.* 1994;269(45):28235–28242.
74. Savaskan NE, Rocha L, Kotter MR, et al. Autotaxin (NPP-2) in the brain: cell type-specific expression and regulation during development and after neurotrauma. *Cell Mol Life Sci.* 2007;64(2):230–243.

## Supplementary Materials

**Figure S1** Time-lapse DIC video of wild type E14.5 mouse retinal neurites growing on laminin under control conditions and then after addition of LPA (100 nM final concentration). <http://www.scripps.edu/mb/chun/birgbauer%20movie.html>

**Abbreviations:** LPA, lysophosphatidic acid; DIC, differential interference contrast.

**Table S1** Total sample size and distribution for analysis of wild type growth cone collapse

Treatment	Growth cones (n)	Collapsed gc (n)	Collapsed gc (%)	Dishes (n)	Mean collapse	SEM	Explants (n)	Diff expts (n)
Control	2970	265	8.9%	14	9.4%	0.9%	101	11
0.1 nM LPA	746	229	30.7%	5	31.7%	7.0%	33	4
1 nM LPA	2189	840	38.4%	14	42.2%	5.0%	102	11
10 nM LPA	1304	1157	88.7%	13	89.4%	1.3%	94	10
100 nM LPA	762	744	97.6%	13	98.2%	0.5%	77	10
1 $\mu$ M LPA	418	415	99.3%	6	98.8%	0.7%	34	5
10 $\mu$ M LPA	532	528	99.2%	5	99.4%	0.4%	39	4
1 nM SIP	501	106	21.2%	3	21.0%	1.2%	24	3
10 nM SIP	366	66	18.0%	3	17.0%	1.5%	22	3
100 nM SIP	527	89	16.9%	3	16.3%	2.3%	25	3
1 $\mu$ M SIP	900	151	16.8%	6	16.3%	2.5%	43	5

**Notes:** Mean collapse rate and SEM is per dish. "Diff expts" indicates independent experiments done on different days, in which each experiment included one or more animals whose retinal explants were pooled for that experiment.

**Abbreviations:** LPA, lysophosphatidic acid; SIP, sphingosine 1-phosphate; SEM, standard error of mean.

**Table S2** Total sample size and distribution for analysis of growth cone collapse from LPA receptor mutant mouse retinal explants

Genotype	Treatment	Growth cones (n)	Collapsed gc (n)	Collapsed gc (%)	Explants (n)	Animals (n)
Wild type	Control	798	67	8%	23	3
Wild type	1 nM LPA	785	217	28%	21	3
Wild type	10 nM LPA	449	386	86%	23	3
Wild type	100 nM LPA	233	227	97%	19	3
<i>Lpar2</i>	Control	877	85	10%	30	5
<i>Lpar2</i>	1 nM LPA	986	244	25%	35	5
<i>Lpar2</i>	10 nM LPA	671	554	83%	34	5
<i>Lpar2</i>	100 nM LPA	483	444	92%	31	5
<i>Lpar1 Lpar2</i>	Control	435	41	9%	16	2
<i>Lpar1 Lpar2</i>	1 nM LPA	404	107	26%	17	2
<i>Lpar1 Lpar2</i>	10 nM LPA	275	208	76%	14	2
<i>Lpar1 Lpar2</i>	100 nM LPA	137	130	95%	14	2
<i>Lpar2 Lpar3</i>	Control	424	49	12%	13	2
<i>Lpar2 Lpar3</i>	1 nM LPA	372	114	31%	16	2
<i>Lpar2 Lpar3</i>	10 nM LPA	355	306	86%	16	2
<i>Lpar2 Lpar3</i>	100 nM LPA	179	174	97%	14	2
<i>Lpar1 Lpar3</i>	Control	151	7	5%	5	1
<i>Lpar1 Lpar3</i>	1 nM LPA	199	65	33%	7	1
<i>Lpar1 Lpar3</i>	10 nM LPA	92	71	77%	9	1
<i>Lpar1 Lpar3</i>	100 nM LPA	36	32	89%	4	1
<i>Lpar1 Lpar2 Lpar3</i>	Control	276	12	4%	9	1
<i>Lpar1 Lpar2 Lpar3</i>	1 nM LPA	147	22	15%	8	1
<i>Lpar1 Lpar2 Lpar3</i>	10 nM LPA	351	313	89%	9	1
<i>Lpar1 Lpar2 Lpar3</i>	100 nM LPA	104	91	88%	8	1

**Notes:** For each genotype, multiple growth cones from multiple explants were analyzed. In most experiments, explants were obtained from multiple animals and analyzed in separate dishes. The wild type animals presented here are littermates of the *Lpar2* animals. Control had no LPA addition.

**Abbreviations:** LPA, lysophosphatidic acid; gc, growth cone.

**Table S3** Sample size and distribution for neurite retraction assay

Genotype	Treatment	Explants (n)	Mean retraction	SEM	Dishes (n)	Animals (n)
Wild type	Control	12	-8.7%	6.1%	5	4*
Wild type	1 nM LPA	17	47.5%	4.2%	6	5*
Wild type	10 nM LPA	20	80.1%	5.9%	9	6*
Wild type	100 nM LPA	25	97.2%	0.7%	9	7*
<i>Lpar2</i>	10 nM LPA	13	81.1%	3.3%	5	4
<i>Lpar1 Lpar2</i>	10 nM LPA	21	78.4%	4.2%	7	6
<i>Lpar1 Lpar2 Lpar3</i>	10 nM LPA	3	63.4%	22.9%	1	1

**Note:** Total number of explants analyzed (n) for each condition along with the mean retraction (%), where negative retraction would be growth, and SEM. In addition, the total number of dishes analyzed as well as the number of animals analyzed for each condition is indicated. \*For wild type analysis, each experiment represented one or more animals whose retinas were removed and explants pooled for analysis; thus, the number of animals indicated is the number of independent experiments, which is a minimum number of animals.

**Abbreviations:** LPA, lysophosphatidic acid; SEM, standard error of mean.

## Eye and Brain

Dovepress

### Publish your work in this journal

Eye and Brain is an international, peer-reviewed, open access journal focusing on clinical and experimental research in the field of neuro-ophthalmology. All aspects of patient care are addressed within the journal as well as basic research. Papers covering original research, basic science, clinical and epidemiological studies, reviews and evaluations,

Submit your manuscript here: <http://www.dovepress.com/eye-and-brain-journal>

guidelines, expert opinion and commentary, case reports and extended reports are welcome. The manuscript management system is completely online and includes a very quick and fair peer-review system, which is all easy to use. Visit <http://www.dovepress.com/testimonials.php> to read real quotes from published authors.